

Comparative study of ZnSe powders synthesized by two different methods and sintered by Hot-Pressing

G. ZHOU, L. CALVEZ, G. DELAIZIR^a, X.-H. ZHANG, J. ROCHERULLE*

Equipe Verres et Céramiques, UMR-CNRS 6226 Institut des Sciences Chimiques, Université de Rennes – France

^aSPCTS, Centre Européen de la Céramique, Université de Limoges – France

ZnSe powders have been synthesized using two different methods: hydrothermal and high energy ball milling. The obtained powders have been dispersed and separated through the ultrasonic process. A comparison has been made between the powders by means of X-Ray powder Diffraction (XRD) and Scanning Electron Microscopy (SEM). The as-prepared ZnSe powders and the fine powders obtained after ultrasonic separation have been sintered by conventional uniaxial Hot-Pressing (HP) technique in order to prepare ZnSe bulk ceramics. The optical properties of the ceramics have been characterized and compared. As a result, the sintering of the fine hydrothermal powder presents the best transparency in the visible and infrared range. The transmission exceeds 60% in the range from 11 to 19 μm .

(Received December 20, 2013; accepted May 15, 2014)

Keywords: Chalcogenides, Chemical synthesis, X-ray diffraction, Infrared spectroscopy, Optical properties

1. Introduction

ZnSe has been widely investigated in the past few years because this II-VI compound has many attractive properties. Presently the most important application field of ZnSe is the fabrication of optical elements for high-power CO₂ lasers [1], but it is also used in designing optical elements for various spectral devices and IR lenses in a broad spectral range from 0.6 μm to 16 μm . Besides that, due to its wide band gap (about 2.7 eV at room temperature), ZnSe also exhibits interesting potential applications in blue-green light emitting diodes, electroluminescent devices, high-density optical storage or thin film heterojunction solar cells [2]. Several routes exist for synthesizing ZnSe nanopowder: solvothermal method [3], hydrothermal method [4] and sonochemical method [5]. Furthermore, chemical vapor deposition (CVD), Bridgman technique [6] or vapor transport method [7] are used to grow bulk ZnSe polycrystal or monocrystal.

Hydrothermal process has been widely used to prepare ceramics materials at elevated temperatures (>80°C) and pressure (>1 $\times 10^5$ Pa) due to its versatility and low energy consumption [8]. All forms of ceramics can be prepared from hydrothermal synthesis, namely powders, fibers, single crystals, monolithic ceramic bodies, and coatings on metals, polymers, and ceramics [9]. High energy ball milling technique is an effective route to prepare different kinds of powders including metallic powder alloys, composites, intermetallics or ceramics which can result in nanocrystalline or amorphous materials [10]. Compared with the traditional powder synthesis, the high energy ball milling process represents a one-step, high-yield, low-temperature and low-cost procedure [11].

Hot-pressing is known as a useful method for preparing many kinds of materials, including metals and

ceramics. It has been used to obtain transparent ceramics in the past decades [12]. To be transparent, the ceramic generally should be poreless and have optically perfect crystal boundaries [13]. Reduced transparency in ceramics is due to light scattering from grain boundaries, birefringence, secondary phases, and residual porosity. Ceramics with a cubic crystal structure and an isotropic refractive index eradicate the optical scattering arising from arbitrary oriented grains [14]. Secondary phases can be avoided by controlling the powder stoichiometry and purity, but also by optimizing the HP conditions. In the same way, additives are used to decrease the content of residual porosity.

In this paper, we expected to find a cheap and simple way to prepare the ZnSe ceramic for optical applications. Hydrothermal and ball milling routes were used to obtain ZnSe powders, followed by an ultrasonic agitation in order to disperse and to separate the fine ZnSe powder from the coarse. The as-prepared powder and the fine powder were sintered using the conventional Hot-Pressing. Powerful techniques such as X-ray diffraction (XRD), Scanning electron microscopy (SEM), Infra-Red spectroscopy, BET technique etc. were used to characterize both the powders and the sintered ceramics.

2. Experimental

2.1 Hydrothermal method

Zn (99.9%, -140+325 mesh, AlfaAesar) powder and Se (99.999%, Umicore) granules are used as reactants and added into a Teflon-lined beaker (20 ml volume) with a molar ratio 1:1. Then, the beaker is filled with 5 mol/l

NaOH aqueous solution up to 70% of the total capacity and introduced in a stainless steel digestion vessel. When sealed, the vessel is placed into an oven and heated at various temperatures up to 200°C with a heating rate of 20°C/min. After soaking for 24 hours, the vessel is taken out and cooled down to room temperature. The products are collected after filtering, and then washed several times by deionized water and absolute alcohol successively. After drying for several hours, the powders are yellow-greenish grains.

2.2 Ball milling method

The same reactants in stoichiometric quantities are introduced into a WC (tungsten carbide) milling jar containing six WC grinding balls. The milling jar is introduced inside the planetary ball miller (Retsch, PM100). The device is stored in a glove box maintained under argon atmosphere and the following milling procedure is applied: rotation cycles of 3min at 300rpm are scheduled with direction reversal and a pause of 3min between each cycle. Sample powders are taken out after 10h, 15h, 20h, 30h, 40h respectively and the reaction rate between Zn and Se is monitored by XRD.

2.3 Ultrasonic agitation

After synthesis, the obtained ZnSe powders are poured into a beaker and immersed in absolute alcohol. Then the beaker is disposed in an ultrasonic apparatus (37 kHz, 140 W) for 5min. The fine ZnSe powders dispersed in alcohol and formed suspended solution. The suspension was collected, centrifuged before being dried in an oven at 70°C for 2h under air ambience.

2.4 Hot Pressing

ZnSe powder (2 g weight) is introduced in a graphite die with a 20 mm diameter. The inner part of the die is lined with boron nitride powder to prevent any adhesion between ZnSe and the mold and also to limit the contamination of ZnSe by the diffusion of carbon from the graphite mold. The temperature is increased to 500°C at 25°C/min under vacuum and held for 30minutes to release the water and others vapors. Then the temperature is increased up to 1050°C with a rate of 15°C/min under nitrogen atmosphere. A pressure of 50MPa is applied during a dwell time of 120min, then the pressure is released and the sample is slowly cooled down to room temperature.

2.5 Characterizations

Densities of the hot-pressed ZnSe samples are determined by the Archimedes' method in deionized water. X-ray Diffraction patterns are recorded at room temperature using the X'Pert Powder (PANalytical) diffractometer equipped with $\text{CuK}\alpha$ radiation ($K_{\alpha 1}, \alpha_2=1.5418\text{\AA}$). The morphology of the samples are observed by Scanning Electron Microscopy (SEM, JEOL JSM-6490). A Micromeritics (Flowsorb II 2300) apparatus is used to determine the specific surface area of the powders by the BET single point method. Before measurement, the samples are dried at 70°C in a oven for more than 12 hours and outgassed under N_2/He flow at 150°C for 30 min. Infrared Spectroscopy analysis is performed using a FTIR (Bruker, Tensor 37) equipment in the range 2.5-25 μm .

3. Results and discussion

3.1 Powders

The powder synthesized by hydrothermal way was dark-yellow. Fig. 1 shows the XRD patterns of the hydrothermal as-prepared powder (HT), fine powder (HTF) and coarse powder (HTC) separated by ultrasonic method. All the main peaks can be indexed by cubic blende ZnSe (PDF No: 37-1463) without any hexagonal wurtzite phase. However additional peaks attributed to zinc metal (PDF No: 04-0831) are still observed in the graph of HT and HTC powder. The reason of existing zinc metal in the powder is as follow⁰: with increasing temperature, some chemical reactions occur in the solution. Se reacts with OH^- first, Se dissolves in the solution as selenious ion. Zn also reacts with OH^- simultaneously, but the reaction is not so active. So ZnSe precipitate on the surface of Zn particles. Small Zn particles can dissolve fast and all react with Se^{2-} to produce ZnSe. But for big Zn particles, there still have metal Zn in the core after the ZnSe precipitated into thick shell which prevents the reaction to proceed. Because metal zinc has higher density (7.14g/cm^3), so the ZnSe grains containing zinc metal have bigger size and higher weight. Heavy and bigger grains can be separated easily by ultrasonic process. This is the reason why zinc metal particles present in HT and HTC powder but not in HTF powder as shown by the XRD patterns in Fig. 1. The SEM pictures of HT powder (a) and HTF powder (b) are showed in Fig. 2. All particles present the cubic structure. The size distribution of particles (Fig. 2a) obtained by hydrothermal method ranges from about 200nm to 3 μm . After ultrasonic process, the HTF powder (Fig. 2b) shows higher homogeneous as the particles size less than 1 μm .

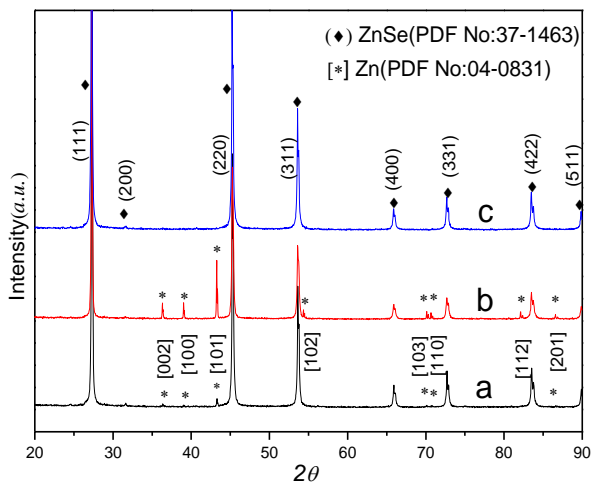


Fig. 1. XRD patterns of powders synthesized by hydrothermal route HT (a), HTC (b), HTF (c).

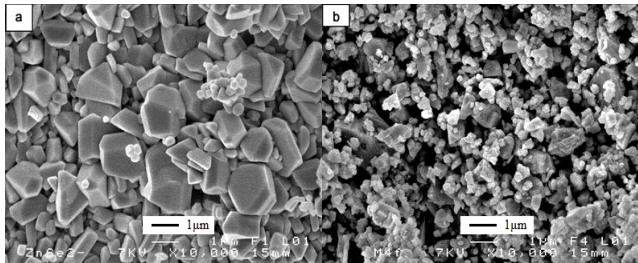


Fig. 2. SEM pictures of HT (a) and HTF (b) powders.

The Fig. 3 presents the XRD patterns of powders synthesized by ball milling of Zn and Se raw elements for different hours. As observable in the Fig. 3 no obvious changes of diffraction patterns occur after 10 hours of reaction demonstrating that chemical reaction between Zn and Se has finished completely after 10 hours milling. Diffraction peaks in Fig. 3 can be attributed to the blende structure ZnSe (PDF No: 37-1463). It also shows that the powders do not contain any hexagonal wurtzite phase, neither metal Zn. Comparing the width of same diffraction peaks in Fig. 1 and Fig. 3, it indicates that the average size of ball milling powder is smaller than hydrothermal powder. In fact, the powders' color changed slightly with increasing milling time. Since the chemical reaction is complete after 10h of milling, this phenomenon might be

due to the change of powders' size and morphology with longer milling time. The morphology character of ball milling-40h (BM) powder and the fine powder separated by ultrasonic method (BMF) was also characterized by SEM as shown in Fig. 2. From the Fig. 2c, one can observe that the BM powder has a broad size distribution and many agglomerates are formed. The size of small particle is estimated to be lower than 50nm, while the large cluster can be more than 5 μ m. In the Fig. 2d, it shows that BMF powder is much more homogeneous than BM powder and the size of main particles is lower than 500nm. Moreover the number of clusters has strongly decreased and all is smaller than 1 μ m. Obviously all particles of ball milling powder do not show any regular structure in the SEM pictures. M. Abdel Rafea synthesized the ZnSe powder using the high energy ball mill with the same type apparatus and observed the introduction of high amount of impurities (27% atom ratio iron) after 15h milling due to the stainless steel jar and balls. The fact we used WC jar and balls can prevent from that contaminate.

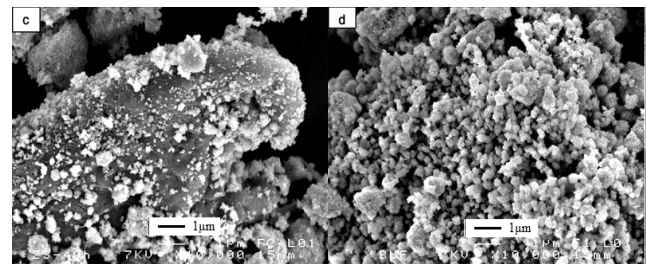


Fig. 3. SEM pictures of BM (c) and BMF (d) powders.

Table 1 lists the particles' surface area measured with different ZnSe powders. As observed, the surface area of the ZnSe powders synthesized by hydrothermal and mechanical milling methods both increased after ultrasonic process since that can get rid of the big size particles. Moreover, the surface area of ZnSe powder obtained by ball milling is larger than the hydrothermal ZnSe powder. That shows the average size of ball milling powder is smaller than the hydrothermal powder. The conclusion is in good agreement with the SEM and XRD results.

Table 1. ZnSe powder characterization.

sample	specific surface area ($\text{m}^2 \cdot \text{g}^{-1}$)	average particle size (μm)	crystallite size (\AA)
HT	1.35	0.84	2576
HTF	2.70	0.42	
BM	8.56	0.13	523
BMF	9.63	0.11	

3.2 Bulk ceramics

The Hot-pressing conditions (temperature-pressure-dwell time) are of a paramount interest to manage the ceramics properties. To obtain transparent ceramic, the structure of ZnSe crystal has to present a cubic lattice and the final ceramic density has to be close to the single crystalline phase. The optimal condition of 1050°C for 2h under 50MPa is chosen after several experiment tests. The ceramic pellets ($\Phi 20 \times 1\text{mm}$) made from powders obtained by the different ways present above are shown in Fig. 4. They exhibit very different color depending on the starting powder. The sample of HTF powder (Fig. 4b) shows red-brown color close to the color of ZnSe obtained by CVD, the other three samples show brown (HF powder, Fig. 4a), dark-yellow (BM powder, Fig. 4c) and black (BMF powder, Fig. 4d) respectively. But for the three samples of HT, HTF and BM powder (Fig. 4a, b, c), each shows different color between the parts of centre and edge due to the non-uniform pressure in the die that causes different rate of compaction between the centre and edge. The XRD graphs (Fig. 5) of the ZnSe ceramics show that all of them are perfectly cubic blende structure and no other crystal phases exist. However one can notice that in the sample of HT powder metal zinc still exists after sintering. These impurities will reduce the ceramic's transparency remarkably because of efficient scattering. The relative densities of HP samples for different ZnSe powders are shown in Table 2 (density of ZnSe single crystal is 5.27g/cm^3). Considering the fact that the ZnSe crystalline phase generated by our method is cubic, the difference of density between the perfect crystalline phase and the one we obtained will indicate the content of pores in the sintered ceramic. From the table, the sample of HTF powder has the highest relative density up to 99.8%, while the sample of BM powder has the lowest. The relative content of residual porosity is $\text{HTF} < \text{BMF} < \text{HT} < \text{BM}$. The SEM pictures (Fig. 6) of the samples' cross section offered good evidences of porosity content. In Fig. 6, one can observe many irregular pores of 1~2 μm size and some small bubbles (<1 μm) existing in the ceramic of BM powder (Fig. 6c). On the contrary, in the sample of HT powder (Fig. 6a) there are many bubbles less than 2 μm dimension but little pores. At the same time, very few pores and bubbles (<1 μm) exist in the sample of HTF powder (Fig. 6b) in good agreement with its highest density. The cross-section of sample with BMF powder presents crystals of small dimension. This might due to the nanoscale size of the starting BMF powder which lead its crystals can't grow larger at present HP conditions.

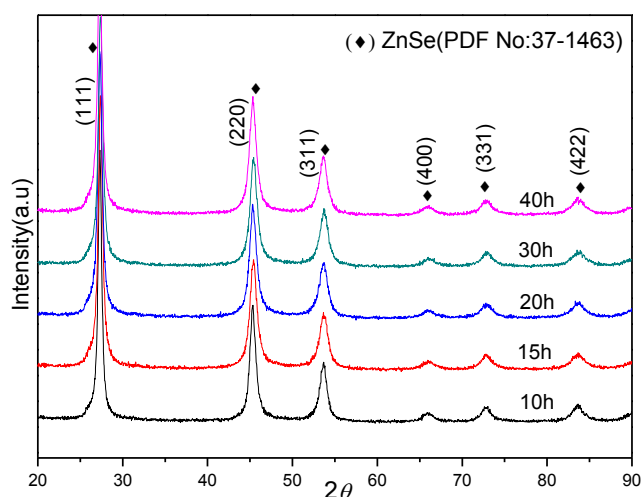


Fig. 4. XRD patterns of ball milled samples obtained after various milling times.

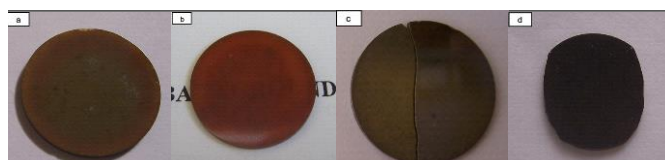


Fig. 5. Bulk sample pictures from different hot-pressed samples (a : HT, b : HTF, c : BM, d : BMF).

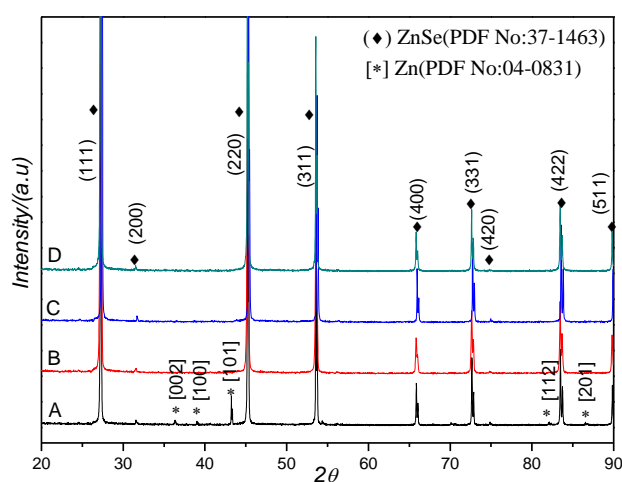


Fig. 6. XRD patterns from different hot-pressed samples (a : HT, b : HTF, c : BM, d : BMF).

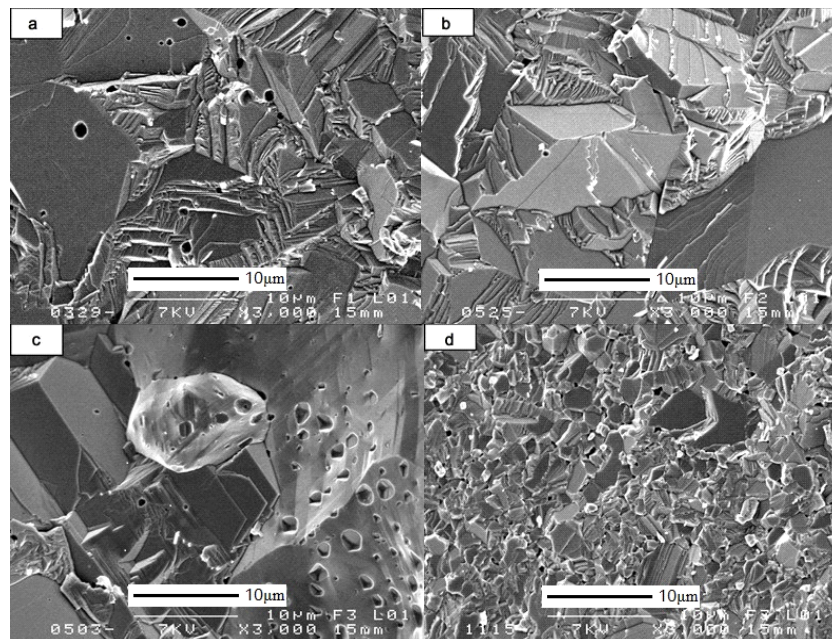


Fig. 7. SEM pictures of different bulk samples (a : HT, b : HTF, c : BM, d : BMF).

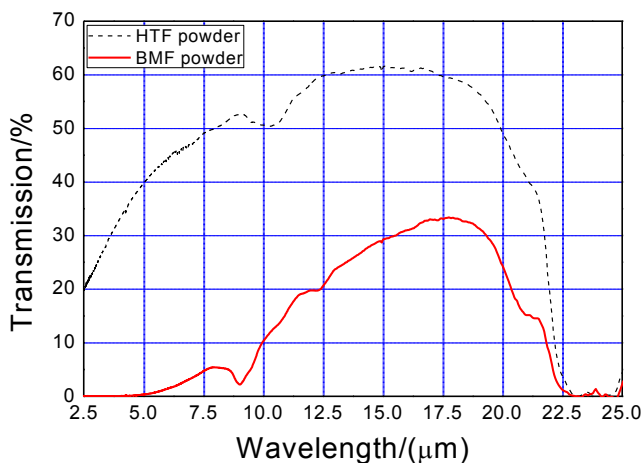


Fig. 8. Transmission spectra of ZnSe ceramics from HTF powder (dotted line) and BMF powder.

Table 2. Hot pressed samples densities and relative densities.

sample	density \pm 0.003(g.cm ⁻³)	relative density \pm 0.05%
a (HT)	5.248	99.58%
b (HTF)	5.261	99.83%
c (BM)	5.140	97.53%
d (BMF)	5.249	99.60%

The two pellets with starting powders before ultrasonic process (Fig. 4a and Fig. 4c) both show absolute opacity in the visible and infrared ranges while two other

ceramics samples sintered with fine powders are transparent in some wave range. The section pictures of different ceramics indicate that pores and bubbles are the most important factors to the opacity. Compared to the fine powder, the less homogenous powder before ultrasonic process might be prone to producing pores and bubbles during the hot-pressing. Besides that, impurities as zinc metal existing in the HT ceramic are also important to its opacity. The sample of HTF powder presents slight transparency in the visible range (Fig. 4b) while the pellet of BMF powder is entirely opaque in the visible range (Fig. 4d), but both are transparent in the infrared range as shown in Fig. 7. The sample of HTF powder presents a good transmission in mid-far infrared range, especial in 10~20 μ m range. Its good transmission mainly benefits from very few pores and bubbles and suitable crystalline cubic structure. Compared with HTF sample, the BMF ceramic shows worse transparency. Besides more pores and bubbles, the fact of the BMF ceramic constituting by small size crystals is another important factor for lowering the transmission. This is because small size crystals will form much more grain boundaries than big crystals which induce higher scatterings at their interface. In fact, one should notice that there still exist carbon contamination in hot-pressing even the graphite die covered by boron nitride. Some black dots due to carbon can be seen on the surface of ceramic samples (Fig. 4). The carbon contamination can also induce serious scattering.

4. Conclusion

Two different synthesis methods, hydrothermal and ball milling, were used to prepare ZnSe powders with a

blende structure. Before ultrasonic agitation, the two powders present very different morphologies. Hydrothermal powder is characterized by a relatively large grain size distribution between 200 nm and 3 μm . On the contrary ball milling powder does not show any regular structure. BM powder has a broad distribution in size from about 0.05 nm to more than 5 μm if we consider the presence of numerous aggregates. After ultrasonic agitation, both the two powders become more homogenous with a typical grain size which is submicronic. Data from XRD patterns and specific surface area values both indicate that the ball milled powder is characterized by a smaller average grain size than hydrothermal powder. All the hot-pressed bulk sample show cubic blende structure, no wurtzite phase were produced during the hot-pressing stage. Pores, bubbles and impurities (zinc metal, carbon etc.) existing in ceramics cause the light scattering which reduces drastically the transparency of the samples. Nevertheless, the ceramic from HTF powder presents a good transmission in mid-far infrared range showing a good efficiency to make optical ceramics using a low cost method of synthesis. The elimination of the residual scattering in the short wavelength, due to diffusion of carbon from the die, will be part of a future work.

References

- [1] E. M. Gavrushchuk, *Inorg. Mater.* **39**, 883 (2003).
- [2] A. N. Krasnov, Y. Purtov, Y. Vaksman, *J. of Cryst. Growth* **125**, 373 (1992).
- [3] H. S. Chen, S. Wang, C. J. Lo, J. Chi, *Appl. Phys. Letters* **86**, 131905 (2005).
- [4] S. Liang, X. Yeming, L. Quan, *Sol. State Com.* **146**, 384 (2008).
- [5] J. Pawlikowski, *Thin Solid films* 127 9-27 (1985).
- [6] Y. D. Li, Y. Ding, Y. Qian, *Inorg. Chem.* **37**, 2844 (1998).
- [7] H. Gong, H. Huang, L. Ding, M. Wang, K. Liu, *J. of Cryst. Growth* **288**, 96 (2006).
- [8] J. Zhu, Y. Kolytyn, A. Gedanken, *Chem. of Mat.* **1**, 73 (2000).
- [9] R. P. Schafer, N. Fukuda, *Materials Science & Engineering R-Reports* **15**, 85 (1995).
- [10] A. Omino, T. Suzuki, *J. of Cryst. Growth* **117**, 80 (1992).
- [11] J. Mimila, R. Triboulet, *Mater. Letters* **24**, 221 (1995).
- [12] Y. Korostelin, V. Kozlovsky, A. Nasibov, P. Shapkin, *J. of Cryst. Growth* **161**, 51 (1996).
- [13] Y. Shu-Hong, *J. of the Ceram. Soc. of Japan*, **109**, S65 (2001).
- [14] K. Byrappa, M. Yoshimura, *Handbook of Hydrothermal Technology*, 755-785 (2001).
- [15] L. Wojciech, R. Suchanek, R. Riman, *Advances in Science and Technology*, **45**, 184 (2006).
- [16] E. Araujo, R. Neto, M. Pillis, F. Ambrozio, *Advanced Powder Technology Materials Science Forum*, **416-4**, 128 (2003).
- [17] C. Suryanarayana, *Mechanical alloying and milling Progress in Materials Science* **46**, 1-184 (2001).
- [18] M. Achimovičová, P. Baláž, T. Ohtani, N. Kostova, G. Tyuliev, A. Feldhoffd, V. Šepelák, *Solid State Ionics*, **192**, 632 (2011).
- [19] C. Chlique, G. Delaizir, O. Merdrignac-Conanec, C. Roucau, M. Dollé, P. Rozier, V. Bouquet, X. H. Zhang, *Opt. Materials* **33**, 706 (2011).
- [20] J. Petit, P. Dethare, A. Sergent, R. Marino, M. Ritti, S. Landais, J. Lunel, S. Trombert, *J. of the Eur. Ceram. Soc.*, **31**, 1957 (2011).
- [21] A. Belyakov, A. Sukhozhak, *Production of Transparent Ceramics Glass and Ceramics* **52**, 14 (1995).
- [22] Z. Seeley, J. Kuntz, N. Cherepy, S. Payne, *Opt. Materials* **33**, 1721 (2011).
- [23] H. Gong, H. Huang, M. Wang, K. Liu, *Ceramics International* **33**, 1381 (2007).
- [24] M. Abdel Rafea, *J Mater Sci: Mater. Electron* **18**, 415 (2007).

*Corresponding author: jean.rocherulle@univ-rennes1.fr